A Study of Space Contamination

by means of

the Surface Plasma Resonance Effect

in Grating Diffraction

NASA Contract NAS 8-25457

by

James J. Cowan

We present here the final progress report on Contract NAS 8-25457, entitled "A Study of Space Contamination by means of the Surface Plasma Resonance Effect in Grating Diffraction". The report is divided into an introduction, a general discussion of results with grating efficiencies and anomalous polarization peak widths, and a summary.

Introduction

The original objective of this study was to investigate, both experimentally and theoretically, the surface plasma resonance effect in diffraction gratings with particular emphasis on the relation of this effect to the space contamination problem in spacecraft using gratings in optical instruments. The theory of surface plasma wave propagation on dielectric-coated metal surfaces, which had been developed earlier[1], was to be applied specifically to cases where a dielectric, in the form of a contaminant, might be deposited on a grating surface and thus change the reflection characteristics of this surface. Experiments were to be done correlating the theory with measurements on grating efficiencies using dielectric coatings similar to those that might be anticipated in practice. It was also intended that the quantum-mechanical theory on photon-plasmon interactions be extended to apply to semi-infinite metal surfaces such as are found with reflecting-type diffraction gratings. These objectives were, for the most part, carried out successfully, as shall be pointed out in the following sections. The experiments were done at the Radiation Physics Section of the Health Physics Division of Oak Ridge National Laboratory.

Efficiency of Dielectric-Coated Concave Diffraction Gratings

Experiments were conducted with two Bausch & Lomb reflecting-type monochromator concave diffraction gratings having aluminum surfaces, a line spacing of 600 lines/mm, and blazed for 1500 A°. The grating calibrator of the Radiation Physics Section was adapted to accommodate a triple polarizer so that efficiencies for both p- and s-polarized light could be measured separately. These gratings were coated with layers of vacuum-evaporated Dow-Corning 705 diffusion pump oil in thicknesses from zero to several hundred A°. The thicknesses were determined at the time of deposition with a quartz crystal monitor. DC-705 was chosen as the contaminant because it is typical of the type of dielectric material that might adhere to a grating surface and because its optical properties are known from independent reflection reasurements made at ORNL.

At the time the efficiency measurements were made a scan was taken of the 1st order diffraction spectrum to observe the anomalous polarization peak wavelength shifts. The wavelength range for the efficiency measurements was from 1000 A° to 2500 A°, because the absorption coefficient of DC-705 has been measured at wavelengths down to 1000 A° and is zero at wavelengths longer than 2500 A°. The diffraction spectrum scan was made in the visible range (4000-7500 A°) because there were no polarization peaks for these particular gratings at shorter wavelengths. The presence of these peaks in the vacuum ultraviolet is often fortuitous and varies from one grating to another. Since the wavelength shift with dielectric thickness is largest for peaks found at shorter wavelengths, the only disadvantage for our purposes was that the thicknesses of oil from zero to about

50 A° could not be determined as accurately as possible.

Figure 1 shows the results of efficiency measurements for a new grating coated with oil thicknesses of zero, 20, 150, and 250 A°. One notes that the decrease in reflectance is most pronounced for small layers (20 A°) at short wavelengths. As the layer thickness is increased (150-250 A), the decrease in reflectance becomes larger at the longer wavelengths. This is in accordance with expected behavior since optical absorption varies inversely with wavelength and directly with the absorption coefficient. (Intensity $\sim (e^{-kx/\lambda})^2$, where k is the absorption coefficient, λ the wavelength, and x the distance the light wave travels in the medium). For DC-705 the absorption coefficient is finite at wavelengths shorter than 2500 A° and reaches a maximum at 1000 A°. There was little overall difference in the reflection for the p- and s- polarizations for a given dielectric thickness, except that s was attenuated slightly more than p at the shorter wavelengths.

The grating coated with 250 A° of oil was left in the vacuum system for 48 hours, and the efficiency measured at the end of this time is shown in Figure 2. The increase in efficiency is attributed to evaporation of the oil at 10^{-6} Torr. Visual inspection of the grating seemed to verify this since thick layers were clearly discernible while thin layers were not. The s-polarized data alone are shown in Figure 3. The anomalous p-polarized 1st order on-blaze spectra of the grating in the visible region are shown in Figure 4. The peaks shift significantly to longer wavelengths for the larger thicknesses while the shift is small for the small layer. One notes that after evaporation the peaks shift back to values characteristic of thin layers. Figure 5 shows the dispersion curve for dielectric-coated aluminum, where $\varkappa$ is the propagation vector of the surface plasma wave. The dotted lines are theoretical values for the dispersion curves for different thicknesses of pump oil on a natural oxide layer of 40 A° using the measured dielectric constants of DC-705. The points are the values of π measured experimentally for the peak near 6000 A°. The dielectric thicknesses corresponding to the crystal monitor readings of 20, 150, and 250 A° are approximately 30. 160, and 250 A°, respectively, which is fairly close agreement. Table I shows the comparison at selected wavelengths between the measured reflectances for different thicknesses, expressed as a percent of the zero thickness value, to the attenuation calculated by the relation (see previous page), Intensity $\sim (e^{-2kt/\lambda})^2$, where here t is the oil thickness. The factor 2 arises because the light wave traverses the oil thickness twice in reaching the detector. One sees that there is fairly good agreement for several of the thicknesses, although the absorption coefficient (and thus the intensity) has larger fluctuations throughout the spectrum than do the experimental values. This crude calculation neglects diffuse scattering other than the diffracted beam.

Figure 6 shows a similar efficiency study made earlier on the second grating. This surface was not new and in fact had been subjected to several vacuum evaporations of other metals before a final aluminum coating was made. Its original reflectance was not as high and a thin oil layer produced a significant change in reflectance. Figure 7 shows the peak wavelength shift for this grating, and the results are similar to those obtained for the first grating.

It is worth mentioning that, although the anomalous polarization peak shifts were measured for p-polarized light, unpolarized light could be used as well. This is because the s-polarized spectra show no anomalous behavior, and for a continuous, unpolarized source spectrum the anomalous peaks would simply appear in the diffraction spectrum superimposed on the continuous background, and thus no polarizers would be necessary if this effect were used for spacecraft instrumentation.

Radiation Damping of Surface Plasmons from Al-Coated Concave Diffraction Gratings

As described in the previous section, grating efficiencies can be monitored by the polarization peak wavelength shift. The dielectric thickness can also be measured by the peak shift if the optical properties of the overcoating dielectric are known. If the optical properties are unknown then only qualitative information about the efficiency and thicknesses can be obtained. It would be very helpful if the optical properties could be found from the anomalous polarization effects.

For a given overcoating metal an unknown real part of the dielectric constant (ε_1) can be determined from the polarization peak wavelengths. If the imaginary part of the dielectric constant, ε_2, could also be measured, one would have complete information on the optical properties of the given metal. We believe this can be done by measuring the widths at half-maximum of the polarization peaks. The widths are due to two effects: radiation damping and electronic damping. Electronic damping is proportional to ε_2 and could be measured directly if the radiation damping were known or could be calculated.

A quantum-mechanical calculation of radiation damping has been performed where consideration has been made of the decay of an intermediate state surface plasmon into a diffracted photon using quantized radiation and plasmon fields and the groove profile geometry in an interaction Hamiltonian. In this picture the incident and diffracted light beams are represented by photons and the surface plasma waves by surface plasmons. The analysis yields a damping or width for a given branch of the experimental data at a given wavelength.

One begins with the quantized photon ($\hat{A}_p$) and plasmon ($\hat{A}_s$) fields, where

$$\hat{A}_p = \sum_{\vec{K}} \int_0^\infty d\eta \left[\frac{4\hbar c^2 \cos^2\theta}{L^2 \omega} \right]^{1/2} \Big\{ \left[\hat{g}_{K\eta}\, e^{i\vec{K}\cdot\vec{\rho}} \right] \Big[\theta(z) \cos\phi \left(i\vec{K} - \frac{K}{\nu} \hat{z} \right) e^{-\nu z}$$

$$+ \theta(-z) \left(i\vec{K} \cos[\eta z - \phi] + \hat{z} \frac{K}{\eta} \sin[\eta z - \phi] \right) \Big] \qquad (1)$$

$$+ g^{\dagger}_{K\eta}\, e^{-i\vec{K}\cdot\vec{\rho}} \Big[\theta(z) \left(-i\vec{K} - \frac{K}{\nu} \hat{z} \right) e^{-\nu z} \cos\phi + \theta(-z) \Big(-i\vec{K} \cos[\eta z - \phi]$$

$$+ \hat{z} \frac{K}{\eta} \sin[\eta z - \phi] \Big) \Big] \Big\}$$

and where

$$\cos\phi = \frac{q}{\sqrt{q^2 + \mu^2 \varepsilon^2}} \qquad \sin\phi = \frac{\mu\varepsilon}{\sqrt{q^2 + \mu^2\varepsilon^2}} \qquad \nu^2 = K^2 + \frac{\omega_p^2 - \omega^2}{c^2}$$

$$q = \sqrt{1 - \mu^2 - \varepsilon} \qquad \mu = \cos\theta \qquad \eta^2 = \frac{\omega^2}{c^2} - K^2$$

and

$$\hat{A}_s = \sum_{\vec{K}} \sqrt{\frac{4\pi\hbar c}{L^2 p_K}} \Big[d_K\, e^{i\vec{K}\cdot\vec{\rho}} \Big\{ \left(i\vec{K} - \frac{K}{\nu} \hat{z} \right) e^{-\nu z} \theta(z)$$

$$+ \left(i\vec{K} + \frac{K}{\nu_0} \hat{z} \right) e^{\nu_0 z} \theta(-z) \Big\} - d^{\dagger}_K\, e^{-i\vec{K}\cdot\vec{\rho}} \Big\{ \left(i\vec{K} + \frac{K}{\nu} \hat{z} \right) e^{-\nu z} \theta(z) \qquad (2)$$

$$+ \left(i\vec{K} - \frac{K}{\nu_0} \right) e^{\nu_0 z} \theta(-z) \Big\} \Big]$$

where

$$\beta_\lambda = \frac{(1-\varepsilon^4)\sqrt{-(1+\varepsilon)}}{\varepsilon^2(1+\varepsilon)} \qquad \nu^2 = \kappa^2 + \frac{\omega_p^2 - \omega^2}{c^2} \qquad \nu_0^2 = \kappa^2 - \frac{\omega^2}{c^2}$$

In these expressions $g^\dagger$, g, $d^\dagger$, d are the creation and destruction operators for photons and plasmons, respectively; ω_p is the plasma frequency; $\vec{k}$ is the propagation vector parallel to the surface, and η , perpendicular to it; $\theta(z)$ is the unit step function; and θ is the photon angle of incidence to the surface.

The interaction Hamiltonian is given by

$$H_{int} = \frac{\omega_p^2}{4\pi c^2} \int d^3\vec{r}\; \hat{\vec{A}}_s \cdot \hat{\vec{A}}_p\, f(\vec{r}) \qquad (3)$$

where $f(\vec{r})$ is a density function that takes into account the variation of the groove profile from a flat surface. This is given by

$$f(\vec{r}) = \begin{cases} \dfrac{n(\vec{r})}{n_0} - 1 & z > 0 \\[2ex] \dfrac{n(\vec{r})}{n_0} & z < 0 \end{cases} \qquad (4)$$

where $z = 0$ is a plane separating the metal and vacuum. $n(\vec{r})$ is the electronic density, which equals n_0 in the metal and zero in vacuum.

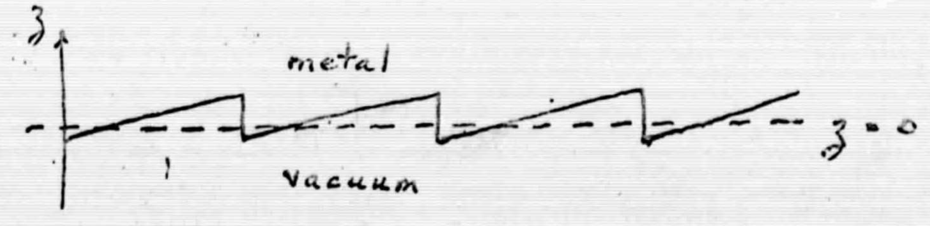

The damping rate for the decay of a surface plasmon into a photon is given by

$$\gamma = \frac{2\pi}{\hbar^2} \left| \langle f | H_{int} | i \rangle \right|^2 \delta(\omega_f - \omega_i) \qquad (5)$$

where f and i are the final and initial states, respectively, and δ is a delta function over the initial and final states. After evaluating eqn. (3) by eqns. (1), (2), and (4) and substituting into eqn. (5) we finally arrive at the following complicated expression for the damping rate

$$\begin{aligned}
\gamma_n = \frac{d^2 \omega_p^4 \cos^8\theta}{2\pi c^2 \rho_k \omega n^2} \Bigg| & \left(\hat{k}_s \cdot \hat{k}_p + \frac{k_s k_p}{\nu_s \nu_p}\right) \cos\phi \\
& \times \Bigg\{ \frac{1}{(\nu_s + \nu_p) d} \left[1 - e^{-(\nu_s+\nu_p) d (1-\sigma)} \right] + \\
& \frac{1}{(\nu_s+\nu_p) d + 2\pi i n} \left[e^{-(\nu_s+\nu_p) d (1-\sigma)} - e^{-2\pi i n \sigma} \right] \Bigg\} \\
& + \frac{\hat{k}_s \cdot \hat{k}_p}{\eta d} \left[\sin(-\phi) - \sin(-\sigma d \eta - \phi) \right] \qquad (6) \\
& + \frac{k_s k_p}{\nu_s \eta^2 d} \left[\cos(-\sigma d \eta - \phi) - \cos(-\phi) \right] - \\
& \frac{1}{\eta^2 d^2 - 4\pi^2 n^2} \Bigg\{ \left(\hat{k}_s \cdot \hat{k}_p \cos\phi - \frac{k_s k_p}{\nu_s \eta} \sin\phi \right) \Big(2\pi i n \cos(-\sigma d \eta) - \eta d \sin(-\sigma d \eta) \\
& - 2\pi i n e^{-2\pi i n \sigma} \Big) + \left(\hat{k}_s \cdot \hat{k}_p \sin\phi + \frac{k_s k_p}{\nu_s \eta} \cos\phi \right) \\
& \times \left(2\pi i n \sin(-\sigma d \eta) + \eta d \cos(-\sigma d \eta) - \eta d e^{-2\pi i n \sigma} \right) \Bigg\} \Bigg|
\end{aligned}$$

where d is the maximum groove depth and the subscript n refers to a particular value of momentum transferred to (or from) the surface plasmon. The n values are related to certain branch values in the experimental data, as shall be shown. The parameter σ, which is a measure of where the z = 0 plane is situated, is found by a separate calculation where one assumes zero forward scattering; i.e., that there is a minimum in the self energy

$$\Delta E = \langle \kappa | H' | \kappa \rangle = \mathcal{H}_{oo} .$$

H' is found by the interaction Hamiltonian,

$$H' = \frac{e\omega_p^2}{4\pi c^2} \int d\tau \, \hat{A}_s \cdot \hat{A}_s \, f(r)$$

using the same $\hat{A}_s$ as before. We find that $\mathcal{H}_{oo}$ is given by

$$\mathcal{H}_{oo} = \frac{\hbar\omega_p^2}{c P_\kappa} \Big\{ \left(1 + \frac{\kappa^2}{\nu_s^2}\right) \left[\frac{1}{d\nu_s^2} \left\{ 1 - e^{-\nu_s d(1-\sigma)} \right\} - \frac{1-\sigma}{\nu_s} \right] + \left(1 + \frac{\kappa^2}{\nu_c^2}\right) \left[\frac{1}{d\nu_c^2} \left(e^{-\nu_c d\sigma} - 1 \right) + \frac{\sigma}{\nu_c} \right] \Big\} \qquad (7)$$

Equations (6) and (7) were programmed on the IBM 360 computer using as input parameters the plasma frequency, dielectric constant $\varepsilon = \varepsilon_1$ of aluminum, and the groove depth and spacing of the concave grating investigated. The value of σ obtained from eqn. (7) enables one to pick out the proper damping rate from eqn. (6). The overall process is described by the diagram

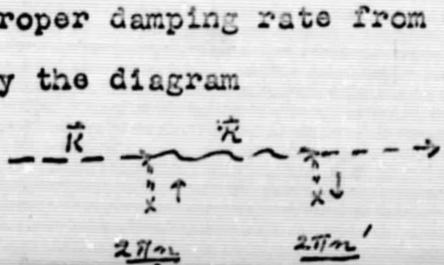

where the surface plasmon exists in an intermediate state between the initial and diffracted photons. δ is the distance between adjacent grooves, and n and n' are integers whose difference is proportional to the momentum transfer at the grating surface. For example, in 1st order diffraction, n'-n = 1; in 2nd order diffraction, n'-n = 2, etc.

Figure 8 shows typical experimental data for the anomalous polarization spectra for different source-detector angles, and the peaks are labeled according to their corresponding n values. One notes that the peaks for the + 1 branch are broader than those for the -4, -5, or -6 branches, and that the + 2 peak has an intermediate width.

The peak widths for the Al-coated grating for different n-values are shown in Figure 9. For clarity only the first three branches are shown. The electronic damping widths, $\Delta\lambda_{elec}$, are found by the relation

$$\frac{\Delta\lambda}{\lambda} \approx \frac{\Delta\omega}{\omega} \approx \frac{\varepsilon_2}{\varepsilon_1^2 + \varepsilon_2^2}$$

where one uses the known dielectric constants for Al. In Figure 10 the electronic damping has been subtracted to leave only the radiative damping widths. The dotted lines are the theoretical widths from eqn. (6), where summation has been made over the possible intermediate state decay scheme for a given diffraction order; for example, for n = 1, we have n' = 2 for 1st order diffraction and the damping rate is $\gamma = \gamma_1 + \gamma_2 + \gamma_{-1} + \gamma_{-2}$. For n = 2, $\gamma = \gamma_2 + \gamma_3 + \gamma_{-2} + \gamma_{-3}$. The theoretical curves are shown for the values n = 1, 2, and 3.

This summation convention appears to be valid, since in the 1st order diffraction spectrum on the opposite side of the reflected beam the n and n' numbers are interchanged, but the widths are identical; i.e., the widths are the same for $n'-n = 3-2 = 1$ for the 1st order (on blaze) on one side and for $n'-n = 2-3 = -1$ for the 1st order (on blaze) on the opposite side for the same source-detector angle.

With this description one observes that as far as general trends are concerned there is good agreement between theory and experiment, especially for $n = 1$ and 2. Hopefully the experimental scatter in the widths can be reduced by taking slower spectral scans that will permit widths to be measured with greater accuracy.

Figures 11 and 12 show peak widths for total damping and radiation damping, respectively, for a Ag coating on the grating, and Figures 13 and 14, for a Au coating. Electronic damping is high for Au in the visible to near ultraviolet region as is apparent from increased peak widths at short wavelengths. Radiation damping for both Au and Ag is seen to be similar to that for Al.

The other experimental work of this study was the construction of a cold trap for the grating to reduce the pressure from 10^{-6} Torr to perhaps 10^{-8} Torr or better. This cold trap consists of a Cu shield of about 7" diameter that encloses the grating. Small holes are provided for the entrance and exit beams and for vacuum evaporations. A 2" diameter pipe that is attached flush against the top of the Cu shield can be filled with liquid N_2 and the reservoir lasts ~ 15 minutes, after initial cooling.

Experiments planned with vacuum evaporated Cd, Mg (and MgO), and Zn were not conducted because one needs a grating with anomalous peaks in the vacuum ultraviolet and, as mentioned earlier, the gratings studied here did not show these effects. However, the dispersion curves were calculated from the known optical constants and are given in Figures 15-17.

Summary

The results of this study indicate that the surface plasma resonance effect can be used effectively to monitor the efficiency of a dielectric-coated grating, the only requirement being an ability to scan the diffraction spectrum so that peak wavelength shifts can be detected.

Studies on the anomalous peak widths show a good correlation between theory and experiment for radiation damping. This means that anomalous polarization phenomena can be used to measure optical constants of metals at wavelengths longer than the plasma wavelength. Hopefully the method can be extended to dielectrics.

References

1. The theory and pertinant equations for the first section of this study have been presented in considerable detail elsewhere, as given in References 2-6.

2. R. H. Ritchie, et al., Phys. Rev. Letters, 21, 1530 (1968).

3. J. J. Cowan, E. T. Arakawa, and R. H. Ritchie, ORNL-TM-2615 (1969).

4. J. J. Cowan, E. T. Arakawa, and L. R. Painter, Applied Optics, 8, 1734 (1969).

5. J. J. Cowan and E. T. Arakawa, Phys, Stat. Sol. (a), April 16, 1970.

6. J. J. Cowan and E. T. Arakawa, Z. Phys., 235, 97-109 (1970).

Table I. Attenuation of intensity from zero oil thickness value determined by experiment (Exp) and by calculation, using absorption coefficient (Calc).

2200 A°

t	Calc	Exp
20	.91	.86
150	.50	.57
250	.32	.34

2000 A°

t	Calc	Exp
20	.77	.87
150	.15	.53
250	.04	.30

1800 A°

t	Calc	Exp
20	.84	.86
150	.27	.52
250	.12	.24

1600 A°

t	Calc	Exp
20	.91	.50
150	.49	.29
250	.30	.15

1400 A°

t	Calc	Exp
20	.96	.23
150	.76	.15
250	.62	.12

1200 A°

t	Calc	Exp
20	.66	.29
150	.05	.11
250	.01	.05

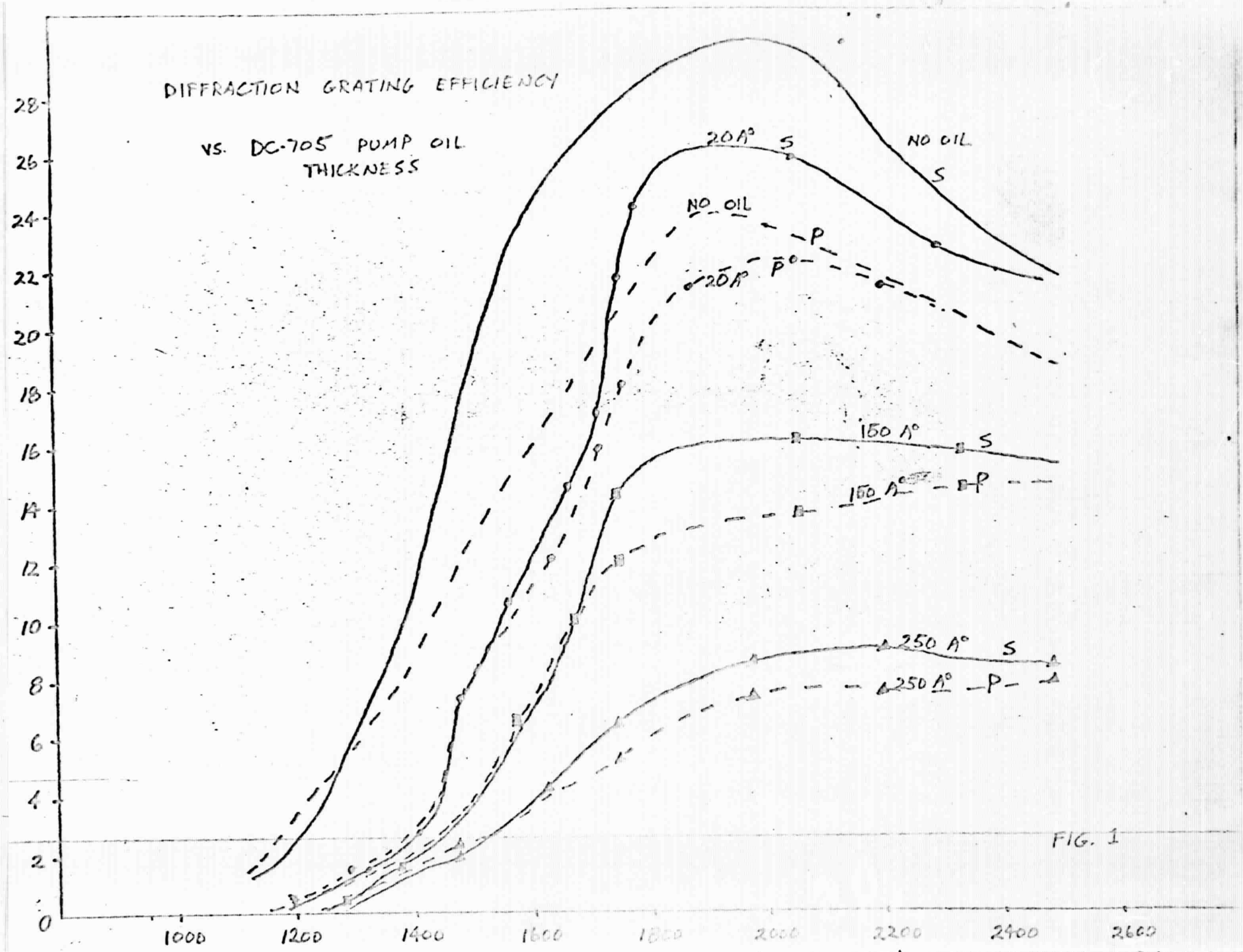
DIFFRACTION GRATING EFFICIENCY
VS. DC-705 PUMP OIL THICKNESS
0
2
4
6
8
10
12
14
16
18
20
22
24
26
28
1000
1200
1400
1600
1800
2000
2200
2400
2600
NO OIL
S
20 A°
S
NO OIL
P
20 A°
P
150 A°
S
150 A°
P
250 A°
S
250 A°
P

FIG. 1

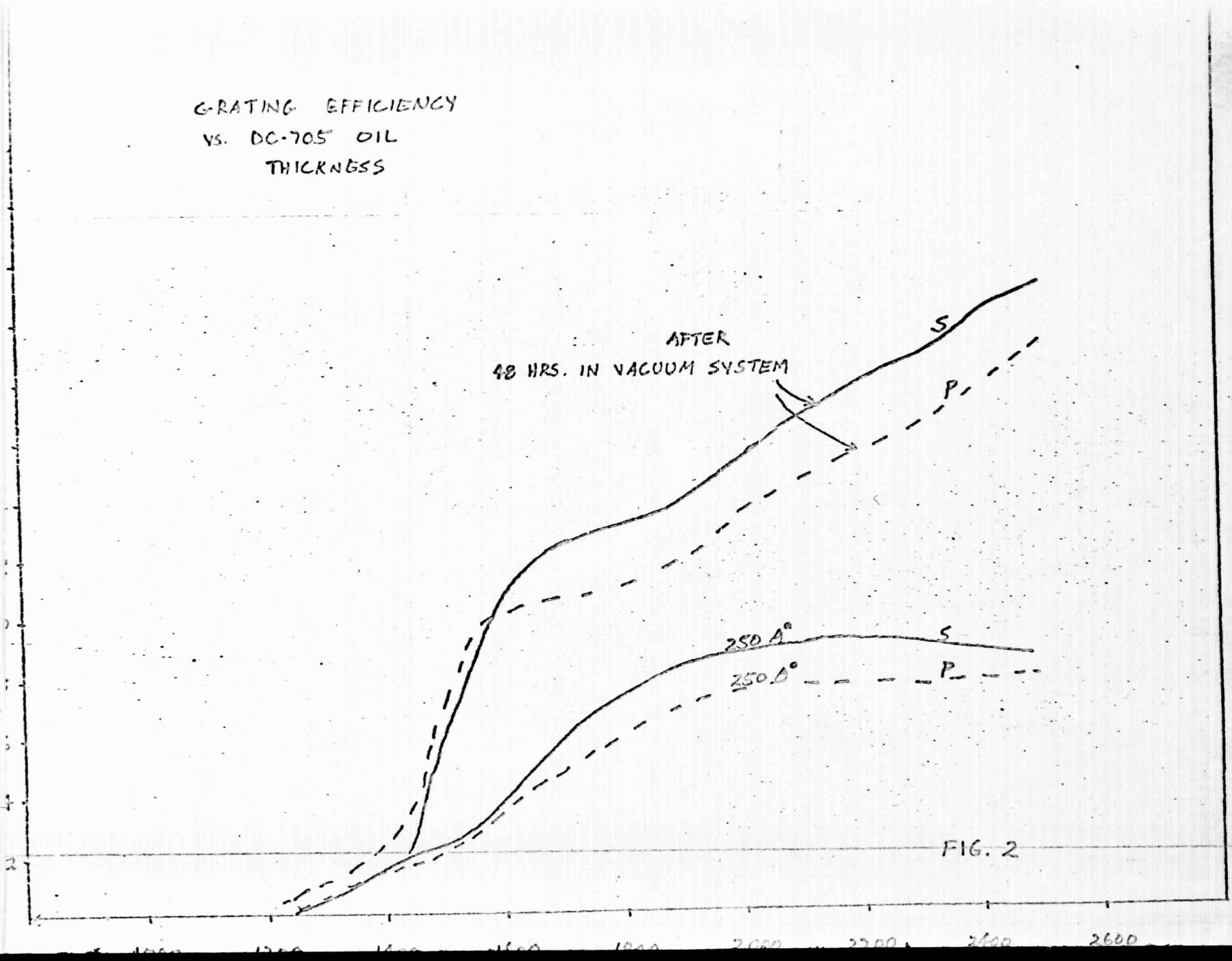
GRATING EFFICIENCY
VS. DC-705 OIL
THICKNESS
AFTER
48 HRS. IN VACUUM SYSTEM
S
P
250 A°
250 A°
S
P

FIG. 2

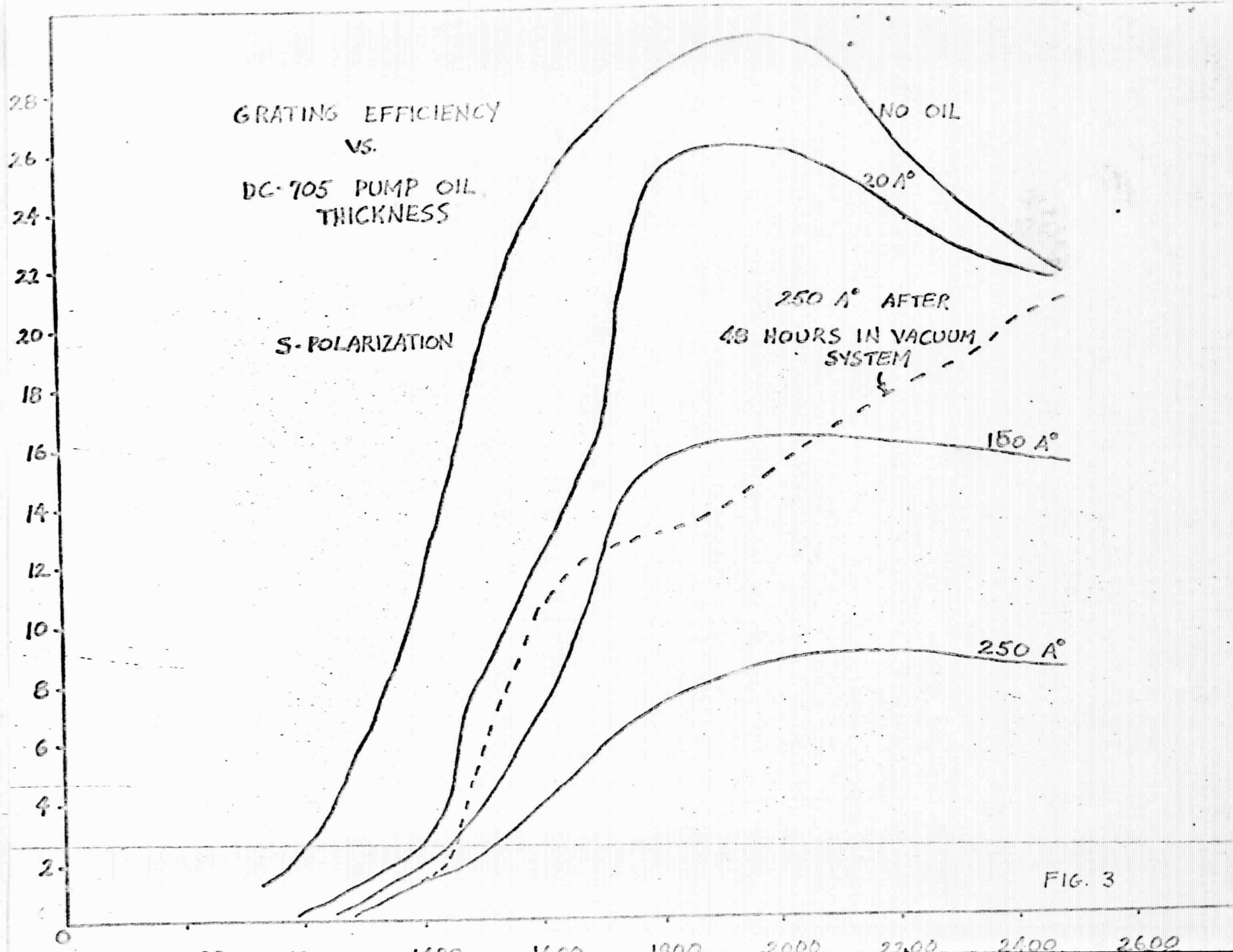
GRATING EFFICIENCY
VS.
DC-705 PUMP OIL
THICKNESS
S-POLARIZATION
NO OIL
20 A°
250 A° AFTER
48 HOURS IN VACUUM
SYSTEM
150 A°
250 A°
28
26
24
22
20
18
16
14
12
10
8
6
4
2
0
2400
2600

FIG. 3

FIG. 4

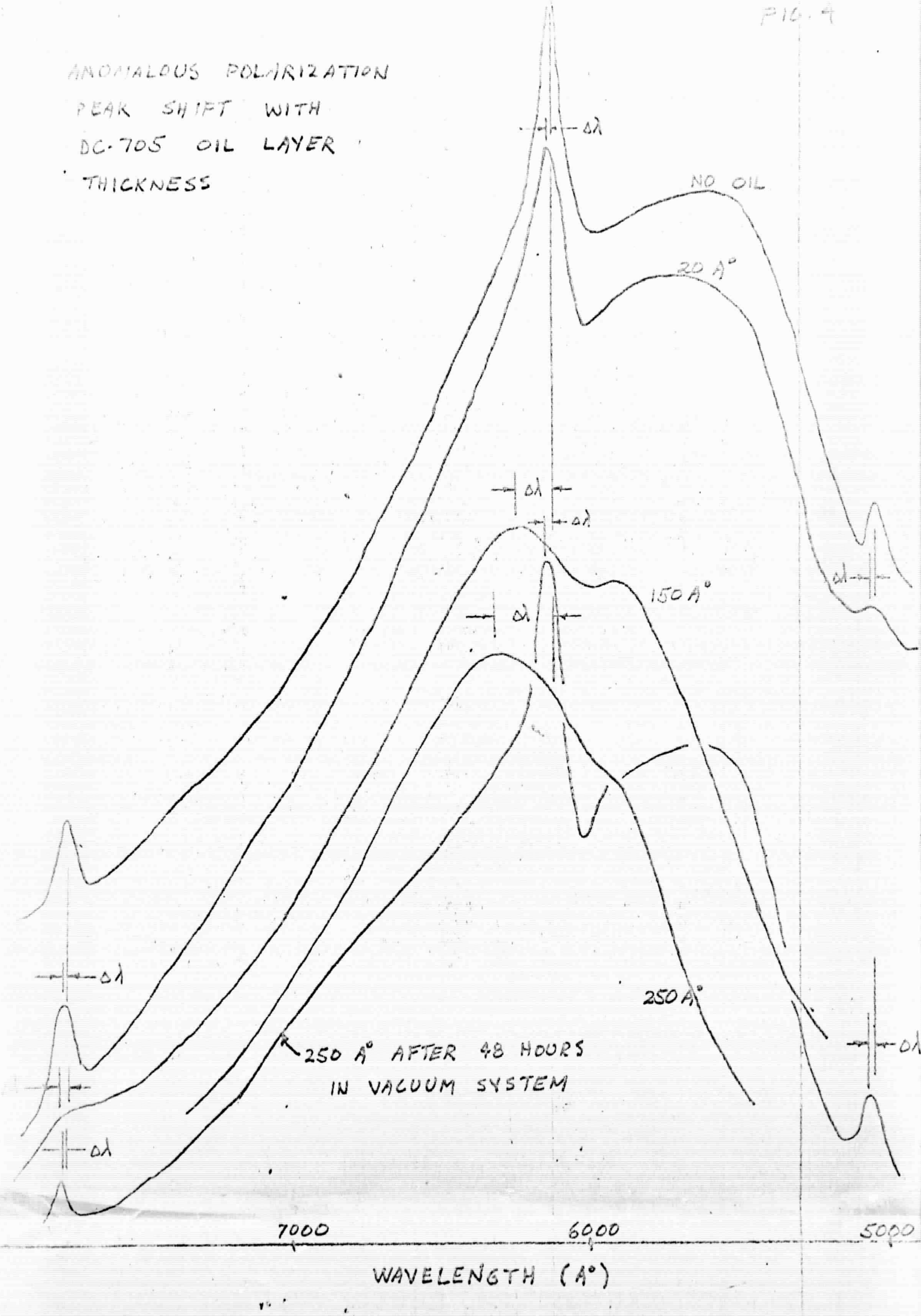

AMOMALOUS POLARIZATION
PEAK SHIFT WITH
DC-705 OIL LAYER
THICKNESS
Δλ
NO OIL
20 A°
Δλ
Δλ
150 A°
Δλ
Δλ
Δλ
Δλ
250 A°
250 A° AFTER 48 HOURS
IN VACUUM SYSTEM
Δλ
Δλ
7000
6000
5000
WAVELENGTH (A°)

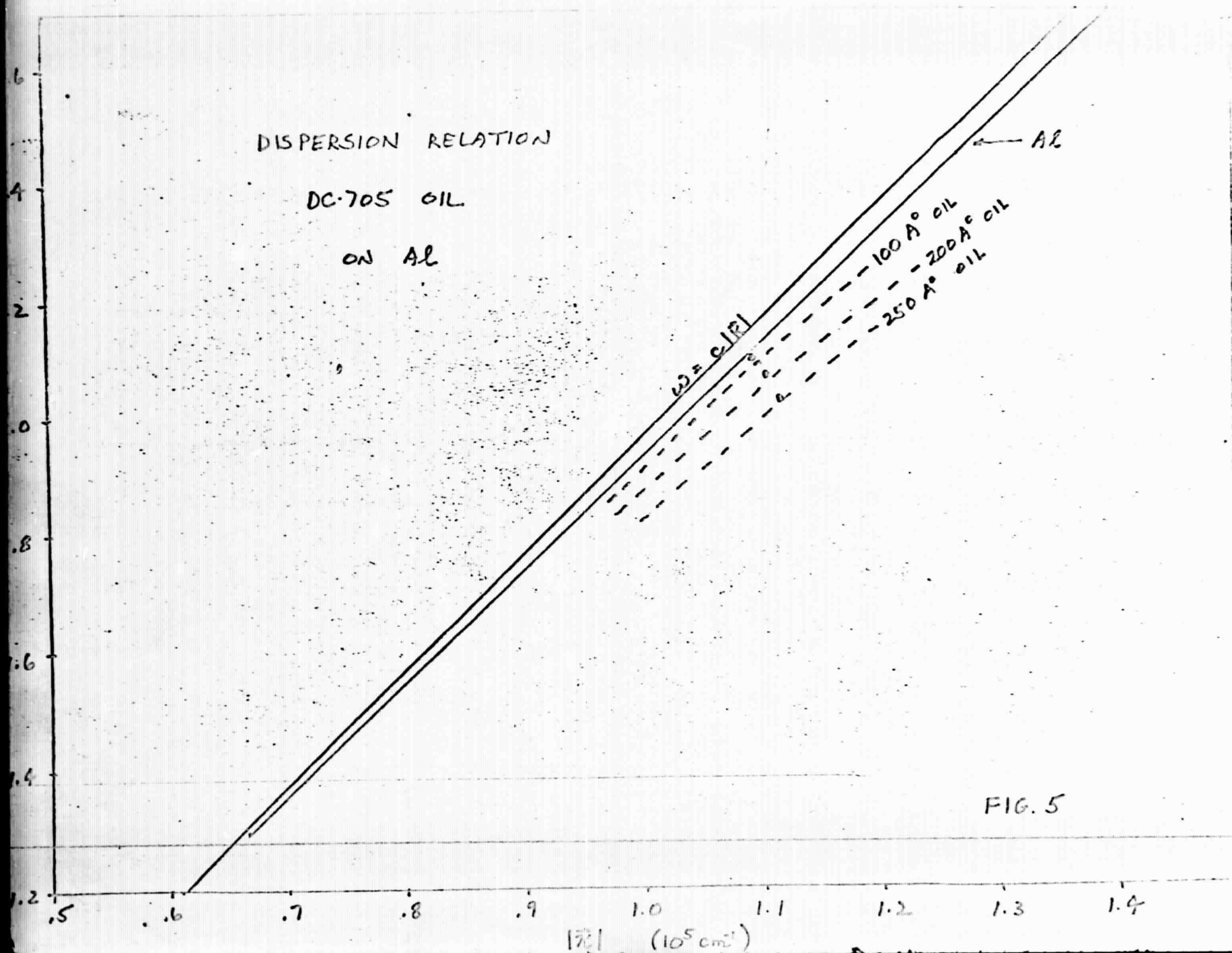

DISPERSION RELATION
DC-705 OIL
ON Al
Al
100 A° OIL
200 A° OIL
250 A° OIL
.2
.4
.6
.8
1.0
1.2
1.4
1.6
1.8
.5
.6
.7
.8
.9
1.0
1.1
1.2
1.3
1.4
(10^5 cm^-1)

FIG. 5

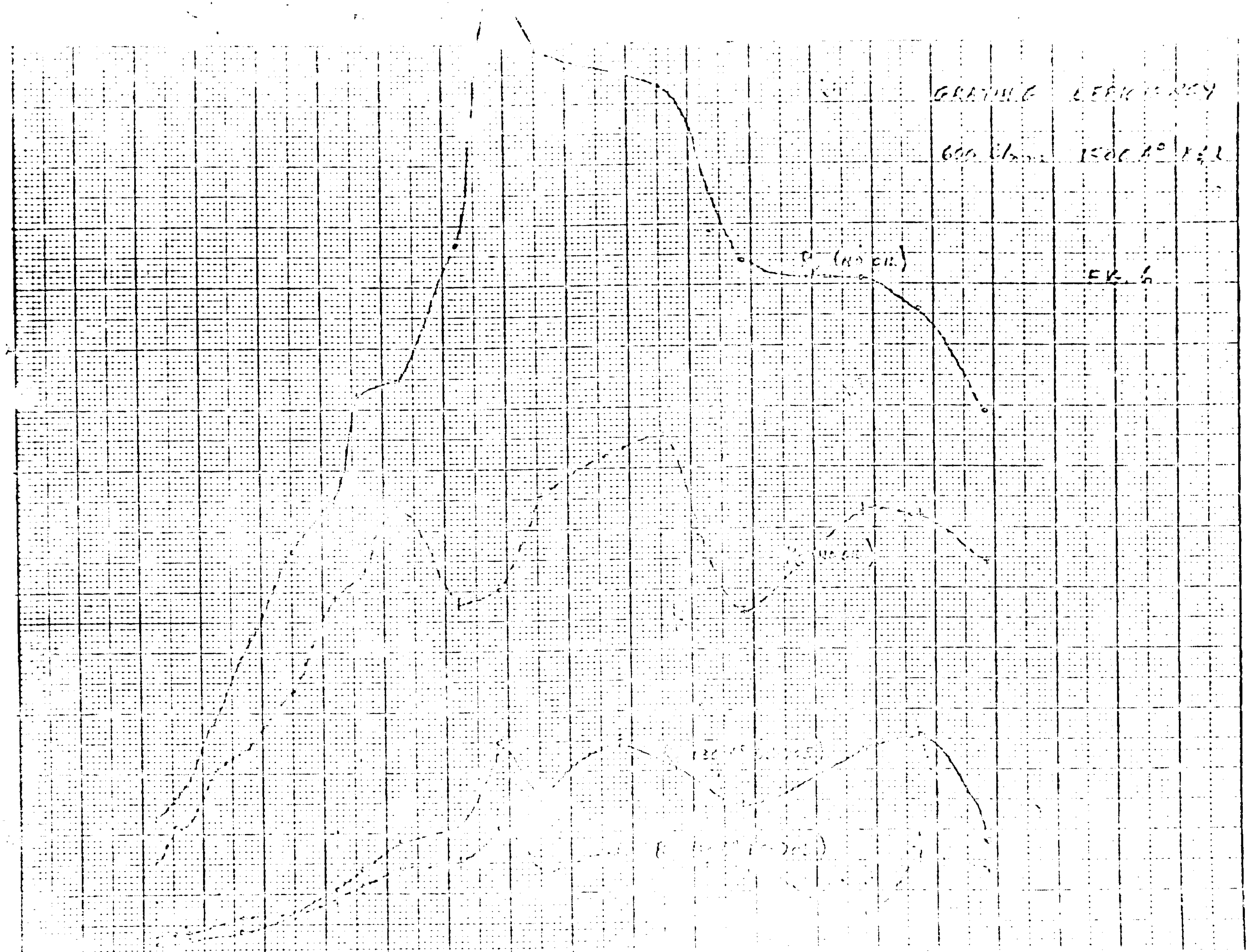

FIG. 6

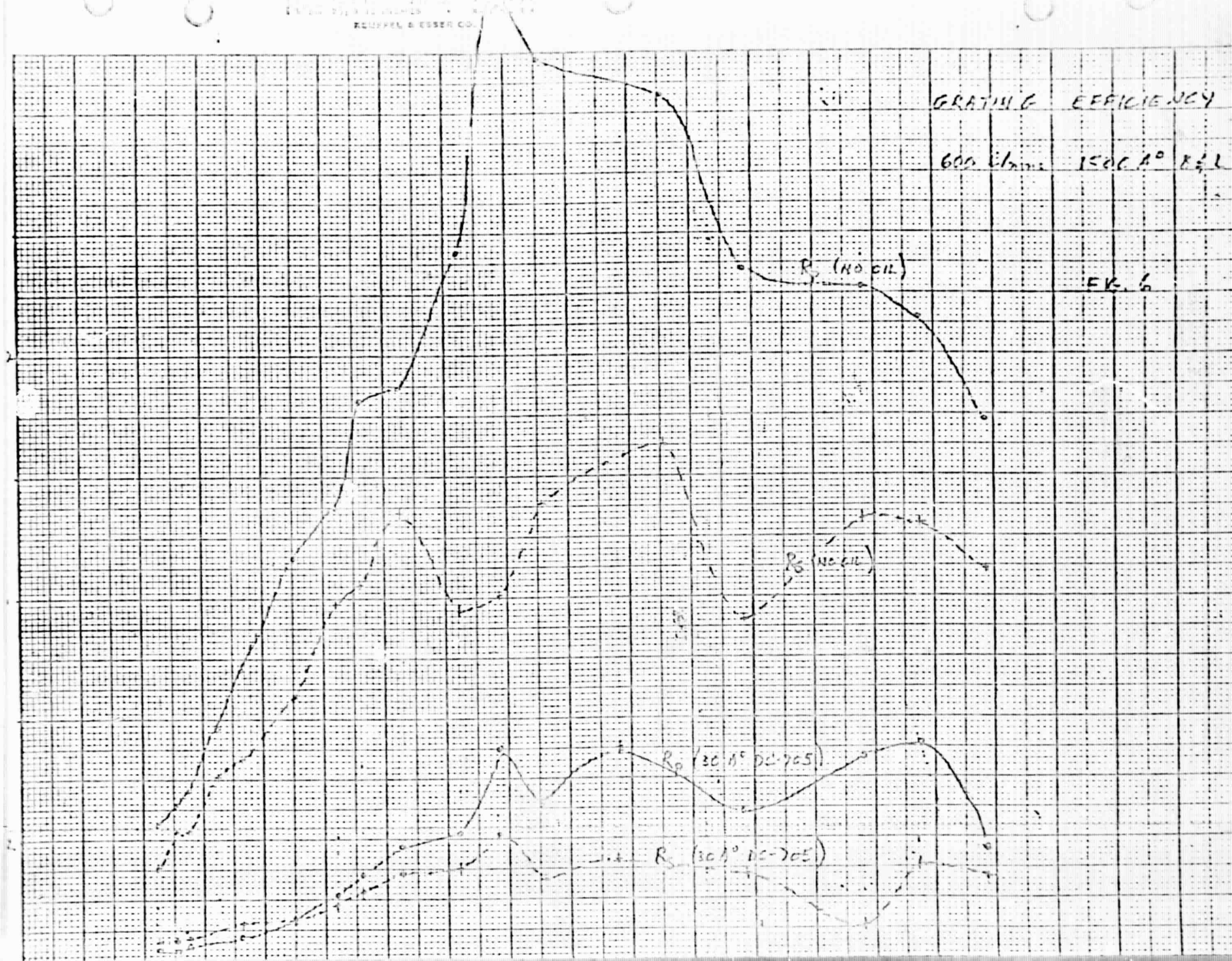
GRATING EFFICIENCY
FIG. 6
(NO OIL)
(NO OIL)
(30 A° DC-705)
(30 A° DC-705)

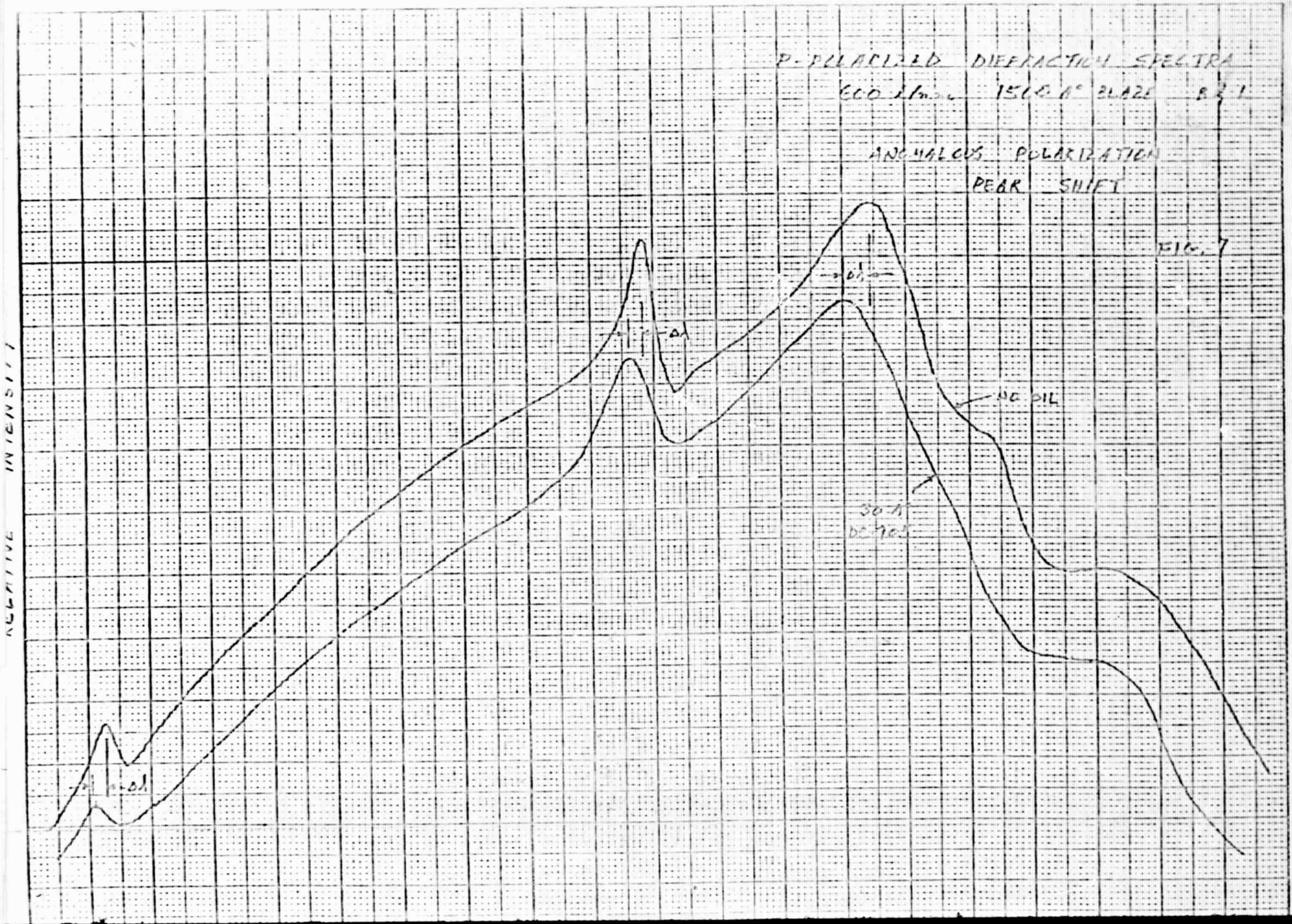
P-POLARIZED DIFFRACTION SPECTRA
ANOMALOUS POLARIZATION
PEAK SHIFT
NO OIL
RELATIVE INTENSITY

FIG. 7

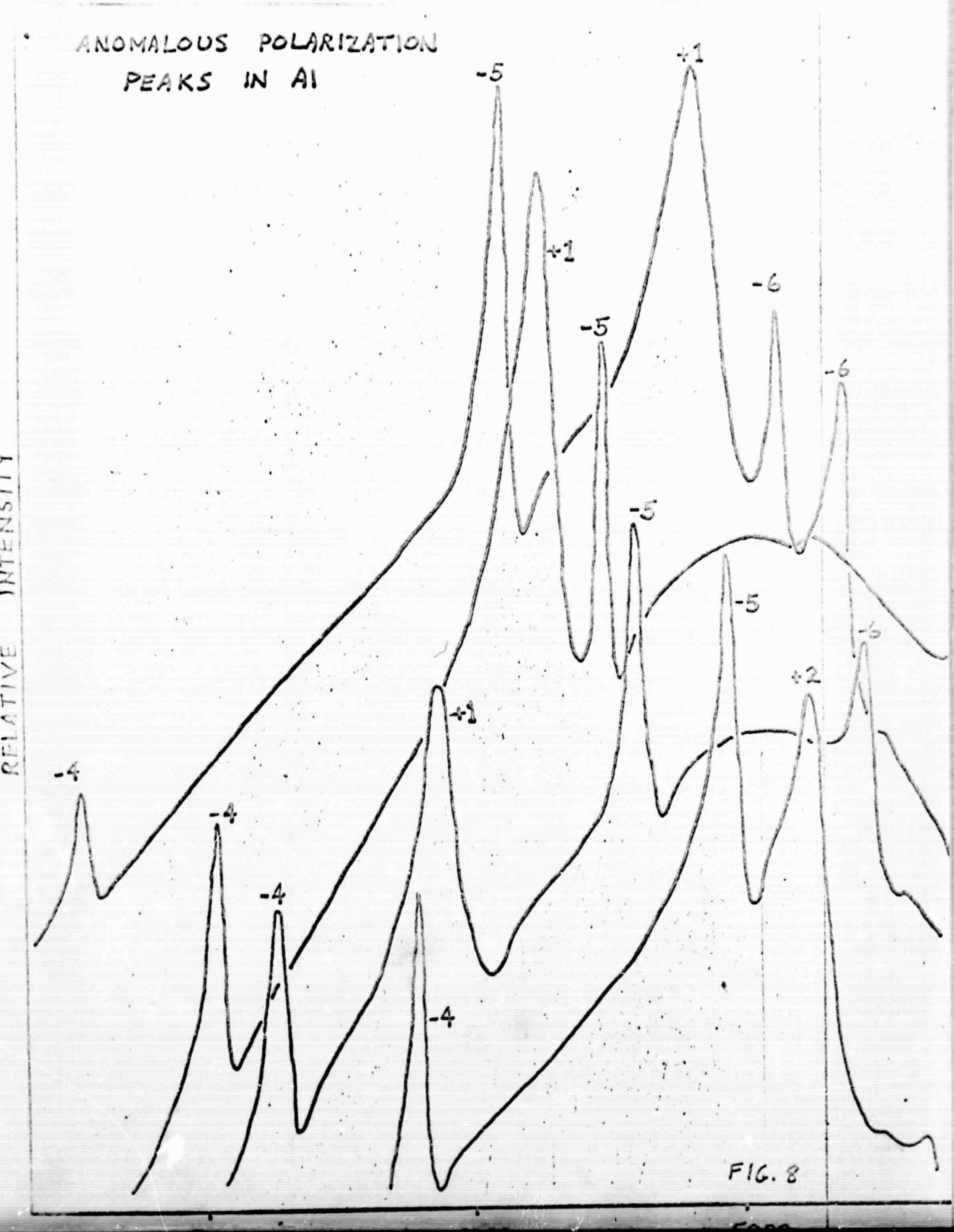

ANOMALOUS POLARIZATION PEAKS IN Al

FIG. 8

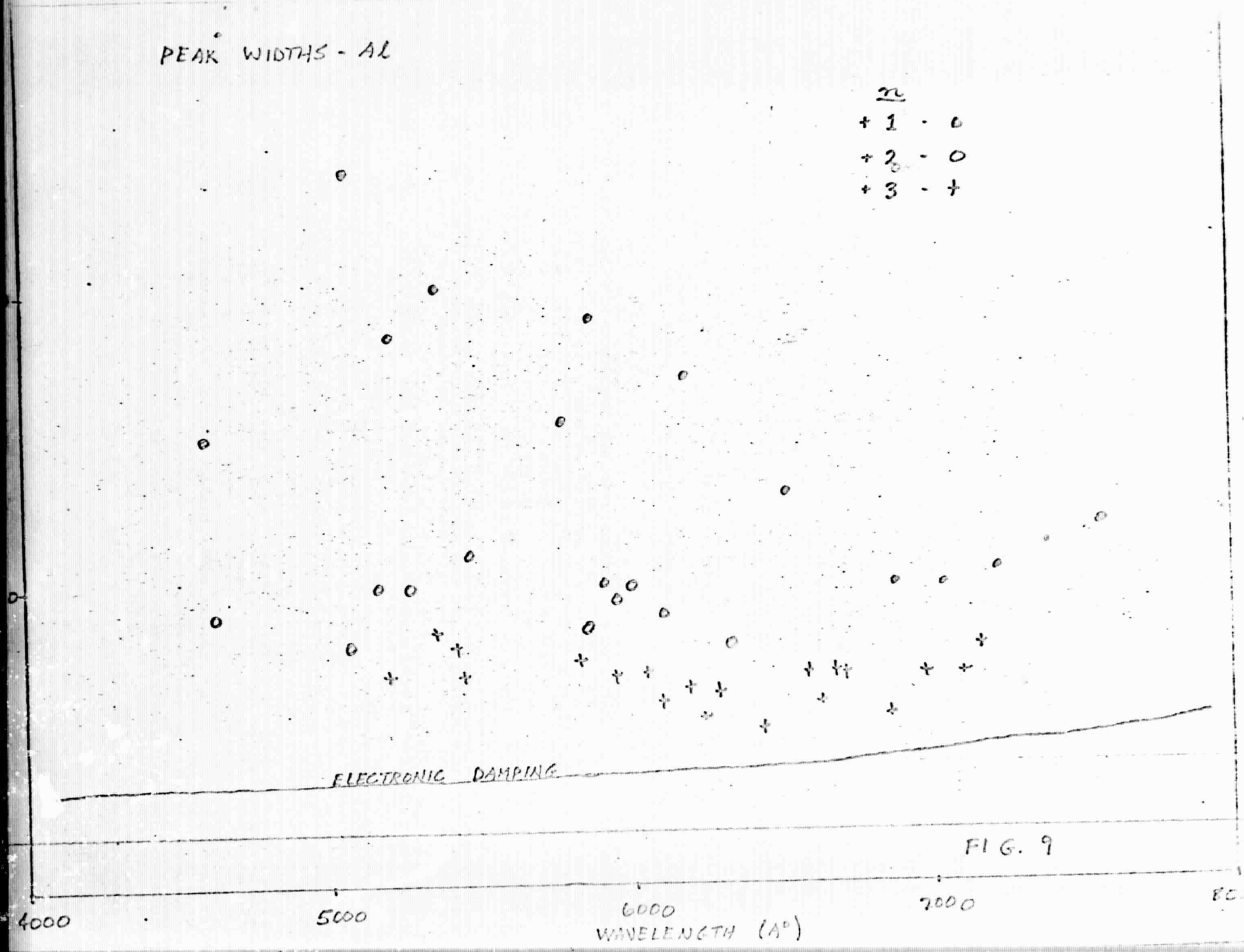
PEAK WIDTHS - Al
n
+ 1 - •
+ 2 - o
+ 3 - +
ELECTRONIC DAMPING
4000
5000
6000
7000
8000
WAVELENGTH (A°)

FIG. 9

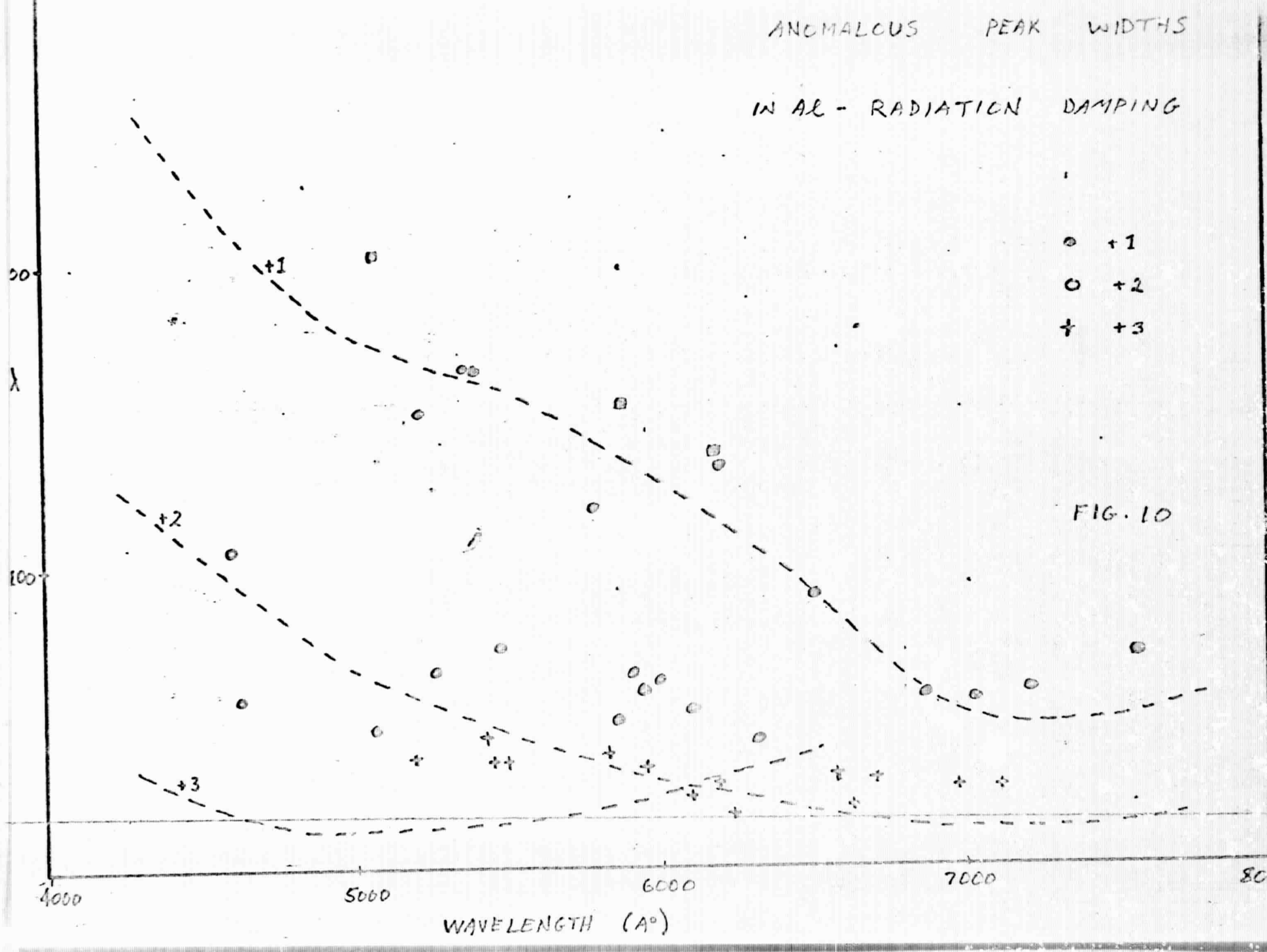
ANOMALOUS PEAK WIDTHS
IN Al - RADIATION DAMPING
+1
+2
+3
200
100
λ
4000
5000
6000
7000
8000
WAVELENGTH (A°)

FIG. 10

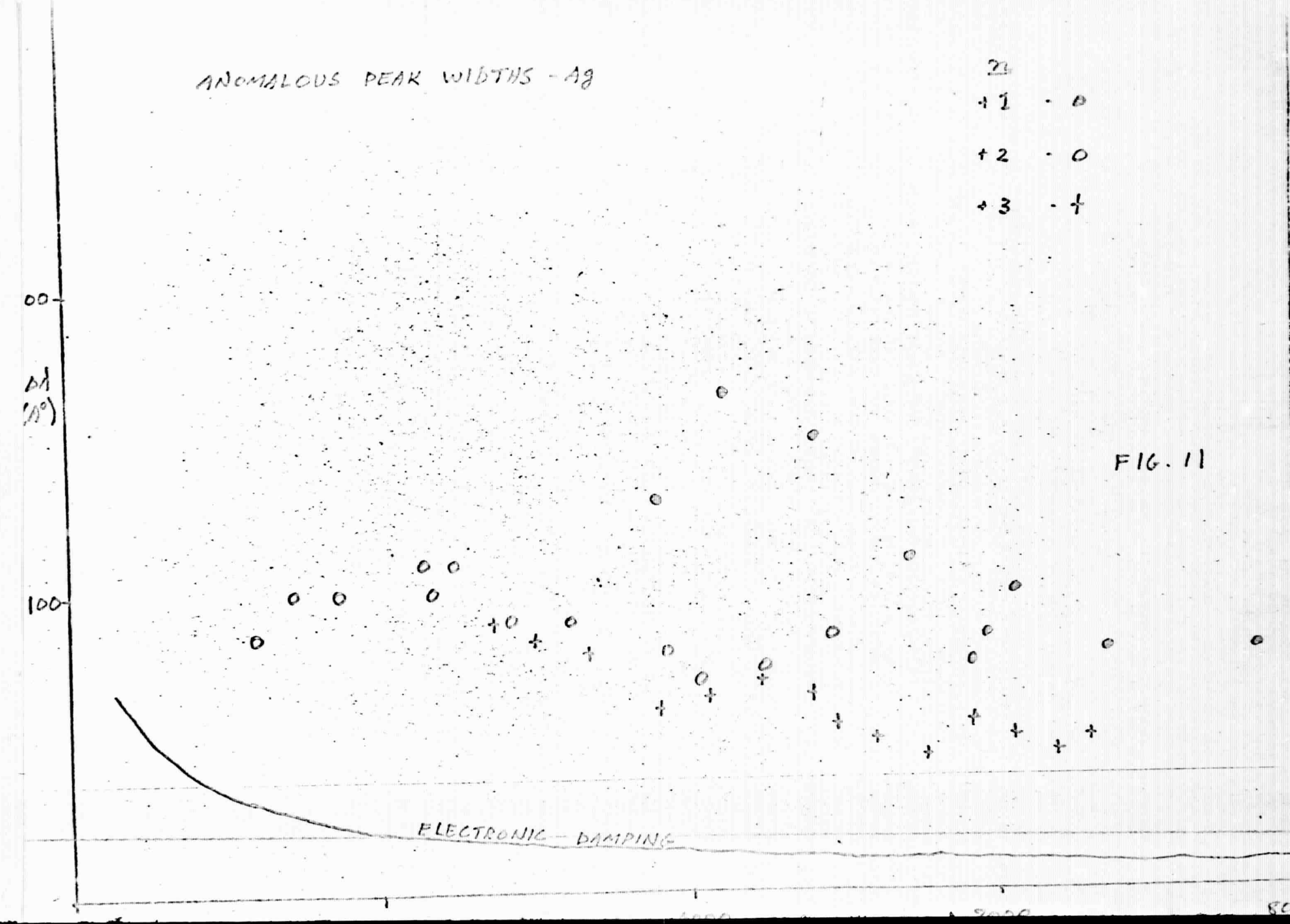

ANOMALOUS PEAK WIDTHS - Ag
n
+1 · o
+2 · o
+3 · +
00
Δλ
(Å)
100
ELECTRONIC DAMPING

FIG. 11

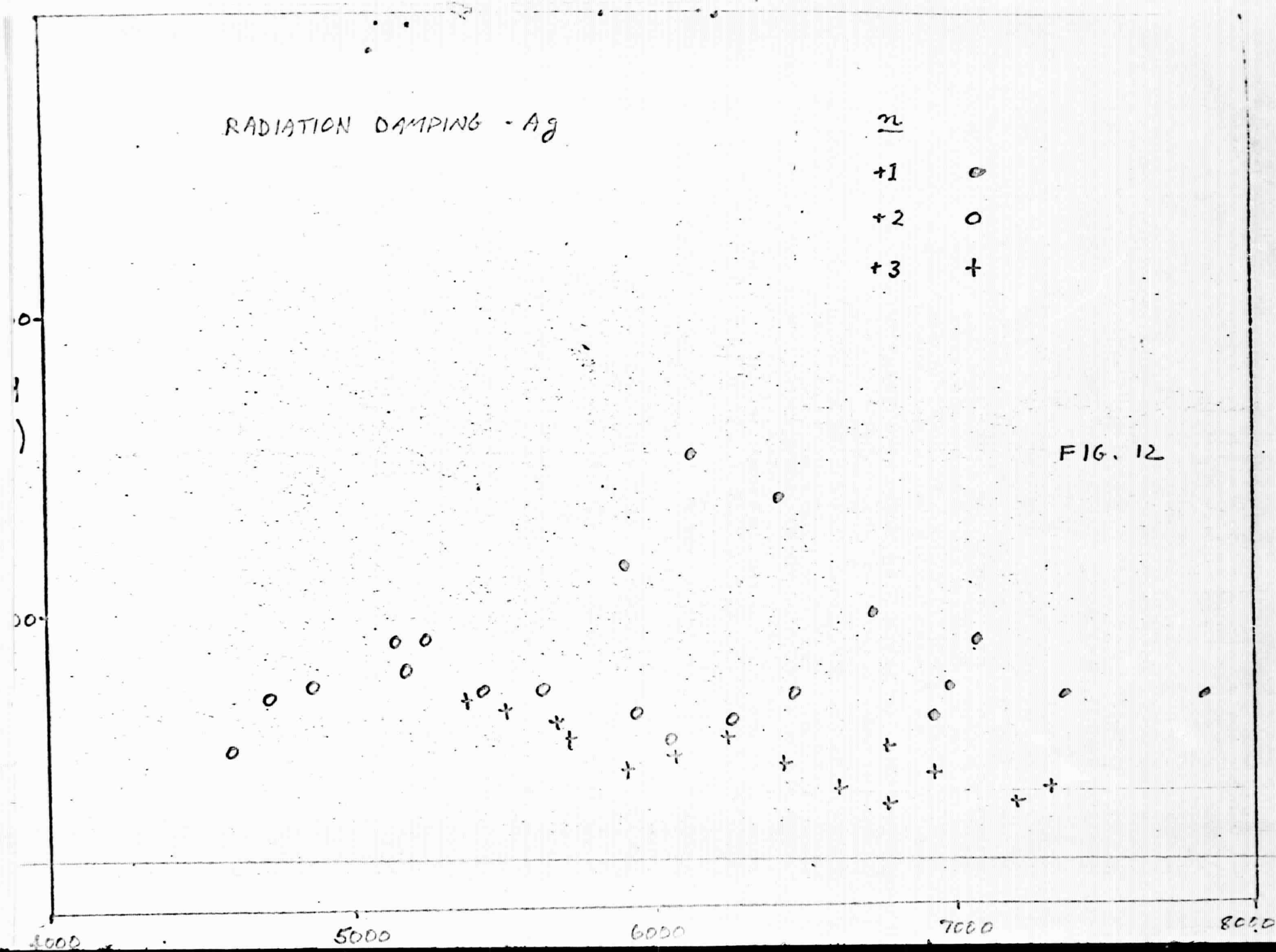

FIG. 12

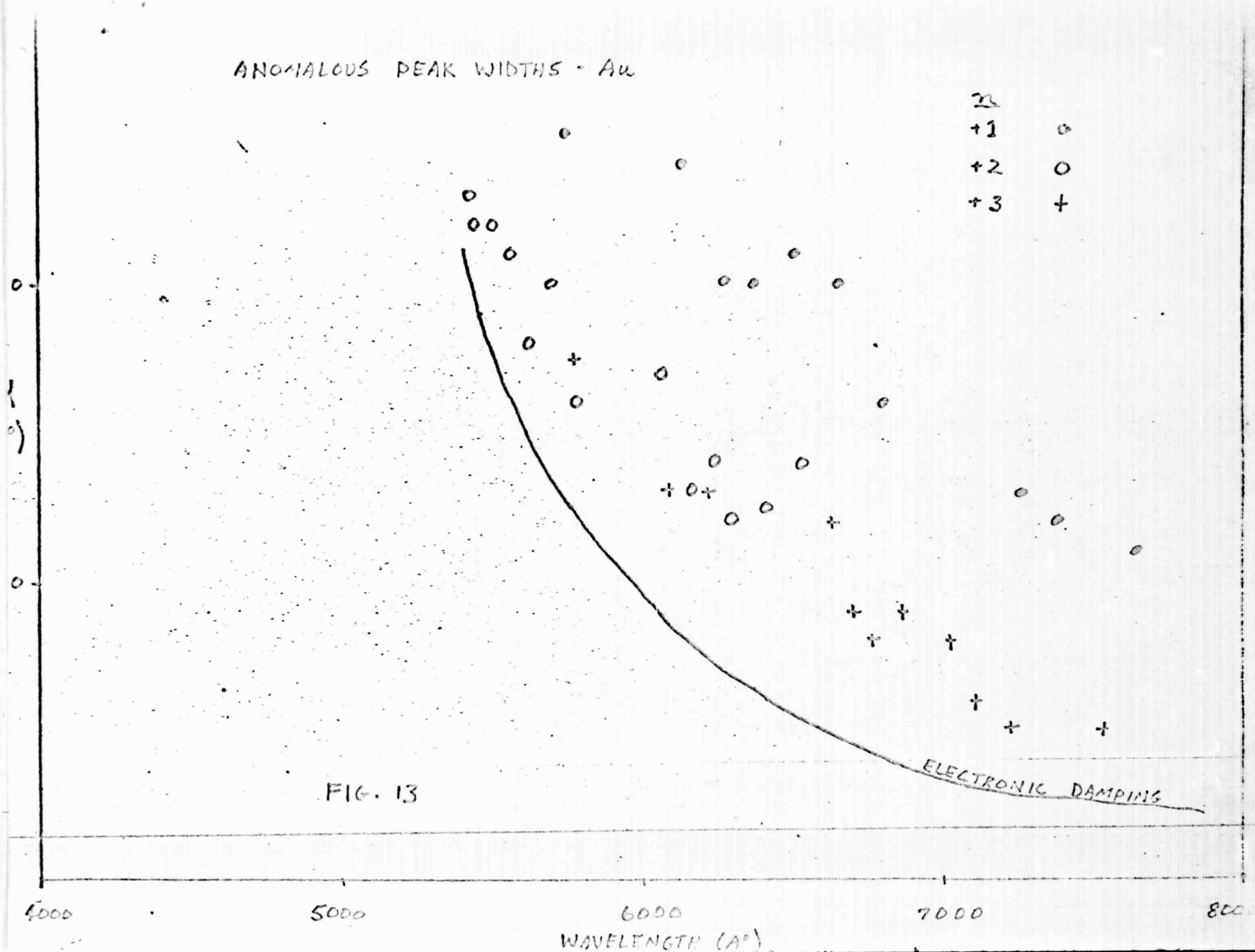

ANOMALOUS PEAK WIDTHS - Au
n
+1
+2
+3
ELECTRONIC DAMPING
4000
5000
6000
7000
WAVELENGTH (A°)

FIG. 13

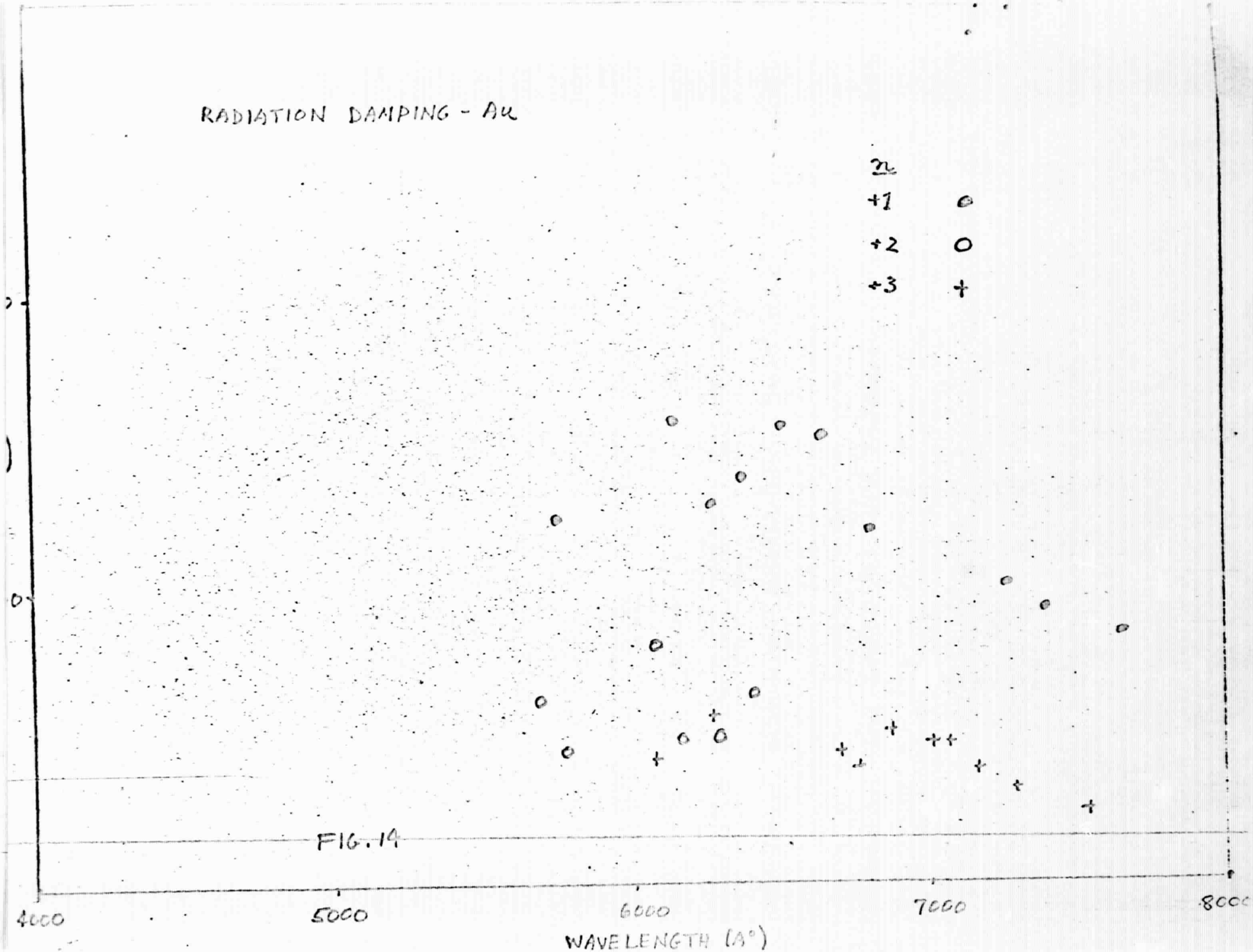
RADIATION DAMPING - Au
n
+1
+2
+3
4000
5000
6000
7000
8000
WAVELENGTH (A°)

FIG. 14

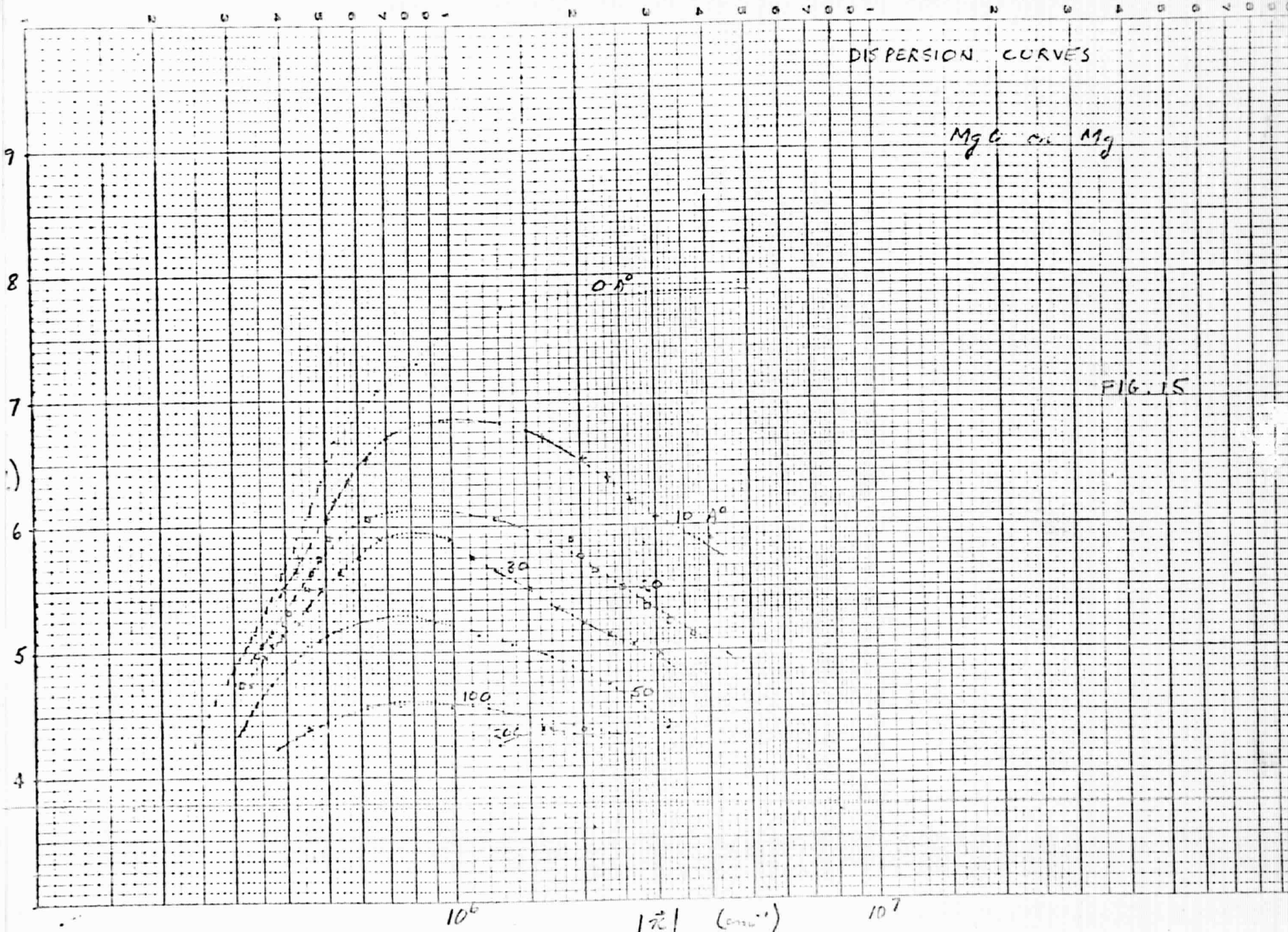
DISPERSION CURVES
MgO on Mg
0.5°
10°
30
50
100
200
9
8
7
6
5
4
10^6
10^7
$|\vec{k}|$ (cm^{-1})

FIG. 15

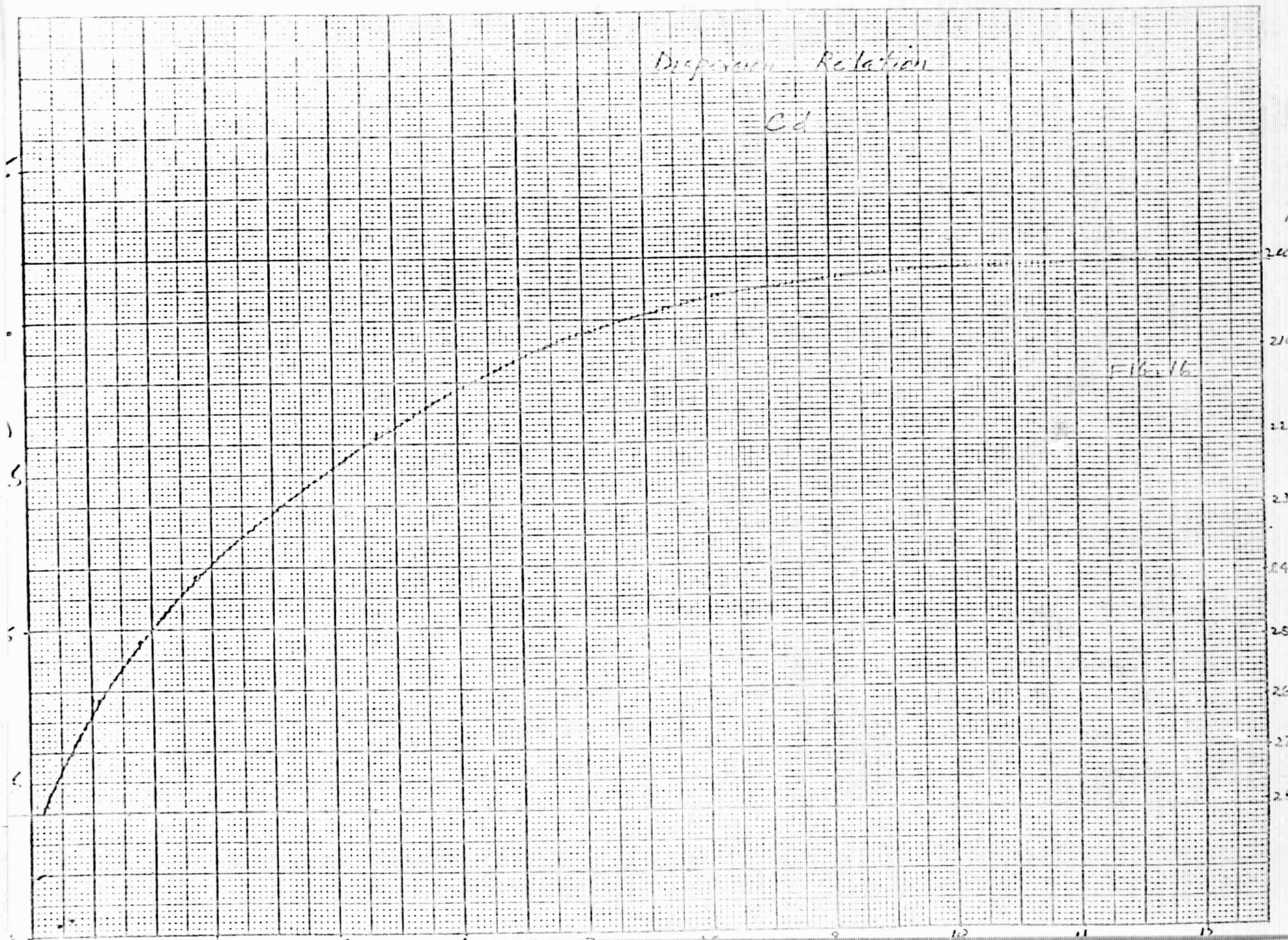
Dispersion Relation
Cd
FIG. 16
220
230
250
260
270
λ

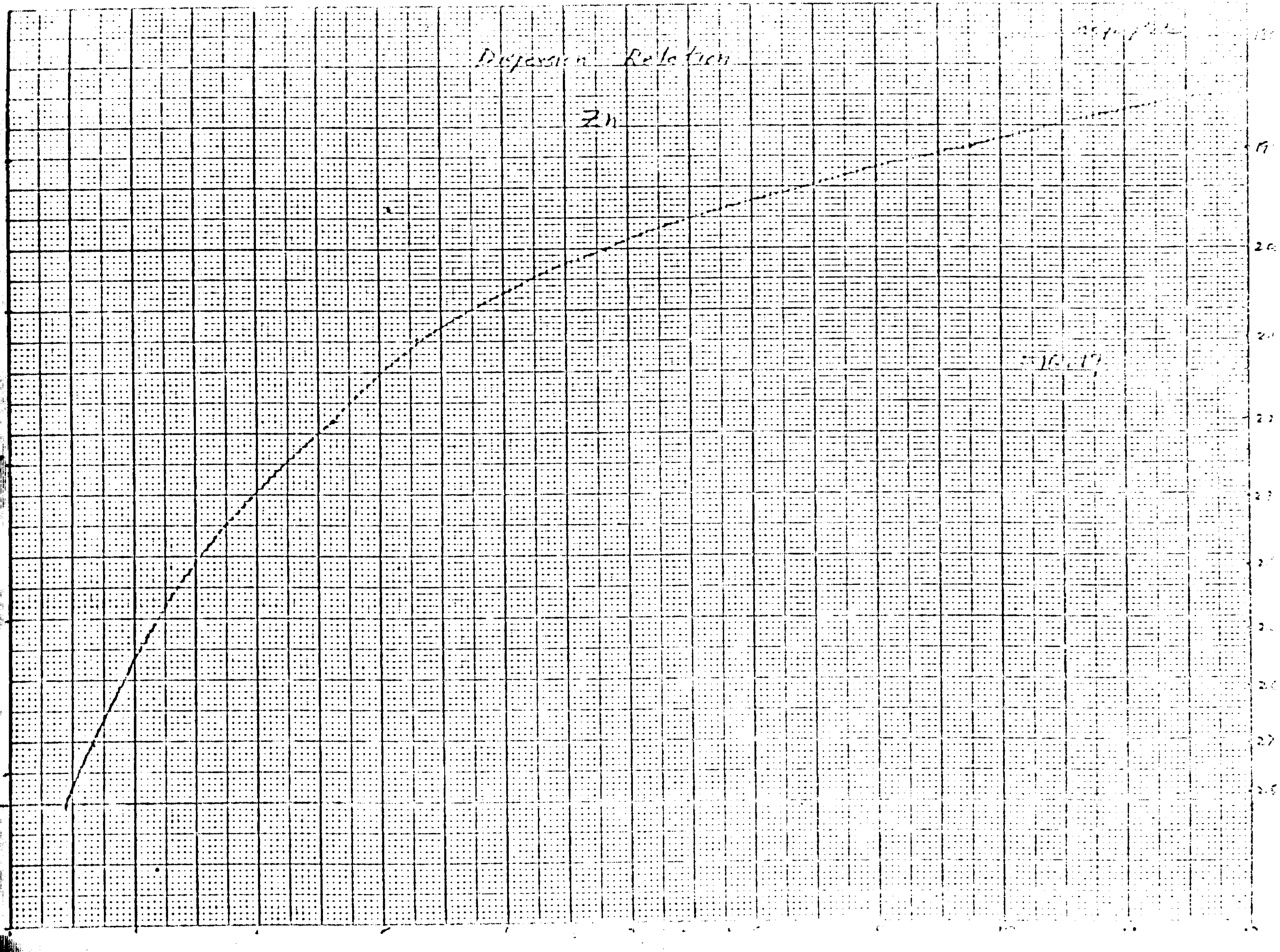
Dispersion Relation
Zn

K+E 10 X 10 TO ½ INCH 46 1470
7½ X 10 INCHES
KEUFFEL & ESSER CO.

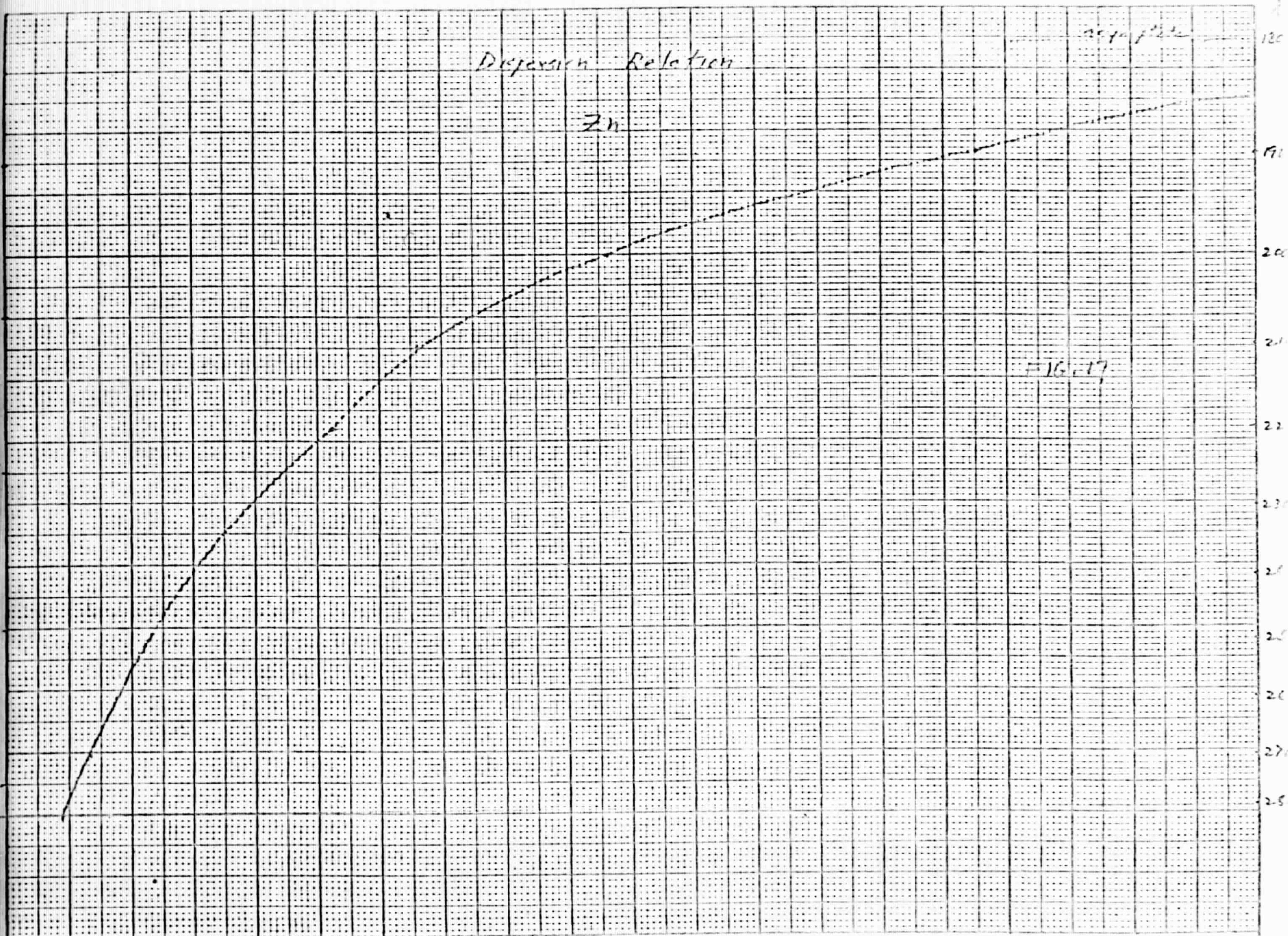

FIG. 17